

Formation of Cellular Solid in Liquid Crystal Colloids

Peter G. Petrov and Eugene M. Terentjev*

Cavendish Laboratory, University of Cambridge, Madingley Road, Cambridge CB3 0HE, U.K.

Received November 28, 2000. In Final Form: February 19, 2001

We investigate aggregation properties of a liquid crystalline colloid formed by dispersing small PMMA particles in thermotropic nematic liquid crystal 5CB. Upon cooling a low-concentration homogeneous mixture below the clearing point of the nematic phase, polymeric particles aggregate into cellular structures, causing enormous mechanical strengthening. We focus on the critical behavior of this system near the isotropic–nematic transition of the liquid crystalline matrix. The initial increase of the storage modulus with decrease of the temperature, signifying the onset of the rigid cellular structure formation, is mapped onto the phase behavior of the colloid. We show that, upon decreasing the temperature, the liquid crystal colloid undergoes two sequential first-order phase transformations. The transition kinetics and the effect of particle size on the resulting mechanical properties of the aggregated colloid are reported and discussed as well.

Introduction

The rich variety of interaction forces is the main cause for the intriguing properties and phase behavior of many classical colloidal systems. Yet, another way to further expand and modify the behavior of colloids is to use a complex fluid, instead of simple liquids, as a suspending medium for colloid particles. When the suspending liquid has a broken symmetry and an associated elastic energy of deformations, the dispersed colloidal particles may produce topological defects in the matrix and cause substantial distortions of the underlying order and long-range elastic forces mediated by it. This is the case when a nematic liquid crystal (LC) is used as a suspending liquid matrix. The large amount of elastic energy stored in the LC leads to profound changes in the phase behavior, the resulting morphology, and the mechanical properties of such systems.

The behavior of a single particle in an LC matrix is now well understood theoretically and studied experimentally. The director field around such a particle is controlled by the competition between the surface anchoring energy, of order $\sim WR^2$, and the Frank elastic energy in the bulk, $\sim KR$ (here R is the particle radius, W is the anchoring energy, and K is the average Frank elastic constant of a nematic phase¹). Strong surface anchoring, $WR/K \gg 1$, makes the director field around the particle incompatible with its uniform distribution in the bulk. As a result, a topological defect is born, confined close to the particle. It can be a line disclination loop like a “Saturn ring” around the particle (of quadrupolar symmetry, Figure 1a)² or a point singularity near it (a dipolar configuration, Figure 1b).^{3,4} Both configurations have been recently observed experimentally.^{4–6} In the case of weak relative anchoring, $WR/K \ll 1$ (which can be achieved, for any values of W and K , by simply reducing the particle size R), the director

configuration can be obtained exactly.² The symmetry of the distortions is quadrupolar, but the director field is only slightly distorted (Figure 1c). Nevertheless, this nonuniform distortion is spreading over long distances from the particle. For typical values of $W \sim 10^{-6}$ J/m² (refs 7 and 8) and $K \sim 10^{-11}$ J/m,¹ the crossover between the topological defect regime and the case of small continuous deformations should be expected for particle radius R between 1 and 10 μ m.

The collective behavior in systems of many colloidal particles, suspended in an LC, is studied much less but is perhaps even more rich in novel physical phenomena. In this case one should expect long-range interaction forces between the particles, mediated by the anisotropic dispersion medium, which arise from the director deformation associated with each individual particle. The very presence of these interactions and their strength would inevitably affect the equilibrium properties and kinetics in such complex colloid systems.

Dispersing particles in an LC medium could be traced back to the early 1970s but has begun to attract growing attention only in the last several years. In their pioneering paper, Cladis et al.⁹ have demonstrated the ability of particles to align along the local director orientation in a cholesteric matrix. They have used it to visualize the director field, their primary concern at the time. However, their results clearly demonstrate that intriguing and reproducible morphologies could be expected in such systems. More recently, Poulin et al.¹⁰ have investigated a mixture of small (60 and 120 nm) particles dispersed in a lyotropic nematic solution. Quenching the system from the isotropic state (where the particles had been homogeneously dispersed in the liquid phase) to a temperature below but close to the nematic transition resulted in phase separation and formation of isolated flocs—particle-rich regions in which the colloid was in a dense liquid or even solid state. A fast quench deep into the nematic region

(1) de Gennes, P. G.; Prost, J. *Physics of Liquid Crystals*; Clarendon Press: Oxford, 1993.

(2) Kuksenok, O. V.; Ruhwandl, R. W.; Shiyankovskii, S. V.; Terentjev, E. M. *Phys. Rev. E* **1996**, *54*, 5198.

(3) Meyer, R. B. *Mol. Cryst. Liq. Cryst.* **1972**, *16*, 355.

(4) Poulin, P.; Stark, H.; Lubensky, T. C.; Weitz, D. A. *Science* **1997**, *275*, 1770.

(5) Mondain-Monval, O.; Dedieu, J. C.; Gulik-Krzywicki, T.; Poulin, P. *Eur. Phys. J. B* **1999**, *12*, 167.

(6) Gu, Y.; Abbott, N. L. *Phys. Rev. Lett.* **2000**, *85*, 4719.

(7) Yokoyama, H.; van Sprang, H. A. *J. Appl. Phys.* **1985**, *57*, 4520.

(8) Lavrentovich, O. D.; Nazarenko, V. G.; Sergan, V. V.; Durand, G. *Phys. Rev. A* **1992**, *45*, R6969.

(9) Cladis, P. E.; Kléman, M.; Piéranski, P. *C. R. Acad. Sci. Paris* **1971**, *273*, 275.

(10) Poulin, P.; Raghunathan, V. A.; Richetti, P.; Roux, D. *J. Phys. II France* **1994**, *4*, 1557.

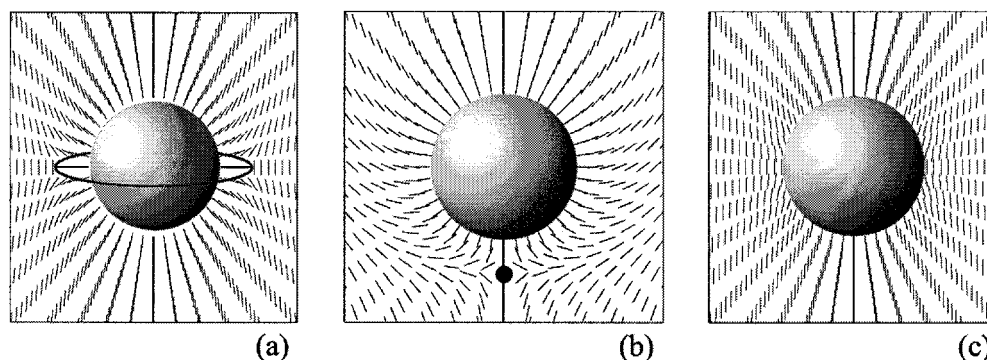


Figure 1. Possible configurations of the director field around a spherical particle immersed in a nematic LC matrix: (a and b) strong homeotropic anchoring; (c) weak homeotropic anchoring.

produced a different morphology—random “solid” strings of aggregated particles, separated from the nematic solvent.

Two recent important studies of collective behavior in liquid crystal colloids should be mentioned here. In the first one, Poulin et al.⁴ have considered dispersion of water droplets in a nematic LC. They have shown the existence of aligned chains of alternating droplets and their corresponding satellite topological defects, due to the long-range attractive and short-range repulsive elastic forces acting between the particle-defect dipoles. Later, the same group explored another system: silica particles (of size 1 μm) dispersed in a cholesteric LC.¹¹ In this case the particle lumped together to form much bigger clusters (flocs on the order of 5–20 μm), which ended up in the nodes of a net of disclinations connecting the clusters. This network was the main cause for the novel mechanical stabilization of the system, raising the storage modulus to about 0.01 Pa at $\omega \rightarrow 0$ and 0.05 Pa at $\omega = 2$ Hz (about three times the value for a particle-free system at the same frequency). This transient state showed aging, with an eventual fate of network disintegration and full phase separation of dense particle aggregates from the LC matrix. In either of these cases, however, the estimated ratio WR/K was large: in ref 11 one should regard R as the size of the particle flocs, which act to distort the LC director field. Thus, this situation leads to topological singularities, strong interaction forces between the particles, and fast phase separation.¹² This, in turn, determines the resulting morphology of the systems. The alternative regime, $WR/K \ll 1$, would ensure that no topological defects are created around the particles and the aggregation forces are moderate. This case has been investigated very recently^{13–15} using small (150 and 250 nm) polymeric particles dispersed in two different nematic liquid crystals, at low concentrations between 3 and 17 wt %. Upon quenching the initial homogeneously mixed colloid from the isotropic to the nematic state, the particles were shown to phase separate and aggregate in thin walls of cellular structure comprising domains of practically pure nematic phase surrounded by walls, in which the particles were densely packed. This metastable, but relatively long-lived rigid cellular structure was the origin of a remarkable enhancement of the mechanical properties of these

systems, increasing the near-equilibrium (low-frequency) storage modulus by several orders of magnitude, up to $\sim 10^3$ to 10^5 Pa.^{13,15} Obviously, a fine balance of kinetic effects is necessary in order to produce such a peculiar morphology. The optimal regime is secured by the small value of WR/K , when the characteristic time scale for the particle aggregation is comparable to the time scale of the nematic nuclei growth during the phase transition.

It is the latter system upon which our present work is based. Here we study in detail the phase behavior and the reversible change of mechanical properties of a liquid crystalline colloid during the formation and consolidation of the cellular structure. Phase transformations are detected by their thermal signature and mapped onto the rheological behavior of the system by measuring the increase of the storage modulus as a function of decreasing temperature. We find that the nematic-to-isotropic transition in the pure nematic liquid is split into two first-order phase transitions in the colloid mixture. The two transitions appear to be related to the onset of the underlying phase separation into particle-rich and particle-poor regions, driven by the nematic mean field, and the subsequent collapse of colloid particles into a dense solid state. We also show a crossover between two distinctive regimes in the kinetic process of the cellular structure formation. In addition, we study the effect of the particle size and the cooling rate on the mechanical properties of the system. Our purpose here is not the material investigation but a study of particular physical phenomena in the critical region of this complex phase transformation. For this reason, we used only one nematic matrix (5CB) and kept constant the particle concentration (5%). In this way one could concentrate on the specific role of nematic order and transition kinetics.

Experimental Section

Materials. Our experimental system is fairly simple. It consists of solid sterically stabilized hydrophobic polymeric particles dispersed at low concentrations in a thermotropic nematic liquid crystal. The liquid crystal, a classical 4'-pentyl-4-cyanobiphenyl (5CB), was obtained from Aldrich and used as supplied. The pure 5CB showed a typical first-order isotropic-to-nematic transition at 35.3 $^{\circ}\text{C}$, as measured by differential scanning calorimetry (DSC). We chose this substance because of its relative chemical stability, well-established properties in the pure state, and convenient transition temperature.

Small monodisperse poly(methyl methacrylate) (PMMA) particles in three lots of different sizes (between 100 and 250 nm; see Table 1) were kindly donated to us by W. C. K. Poon (University of Edinburgh) and V. J. Anderson (Van't Hoff Laboratory, Utrecht University). They were sterically stabilized by grafting poly-12-hydroxystearic acid (PHSA) chains. In addition to sterical stabilization, the grafted polymer ensured a homeotropic alignment of the liquid crystal on the surface of the

(11) Zapotocky, M.; Ramos, L.; Poulin, P.; Lubensky, T. C.; Weitz, D. A. *Science* **1999**, *283*, 209.

(12) Terentjev, E. M. In *Modern Aspects of Colloidal Dispersions*; Ottewill, R. H., Rennie, A. R., Eds.; Kluwer Academic Publishers: Dordrecht, The Netherlands, 1998; p 257.

(13) Meeker S. P.; Poon, W. C. K.; Crain, J.; Terentjev, E. M. *Phys. Rev. E* **2000**, *61*, R6083.

(14) Anderson, V. J.; Terentjev, E. M.; Meeker S. P.; Crain, J.; Poon, W. C. K. *Eur. Phys. J. E* **2001**, *4*, 11.

(15) Anderson, V. J.; Terentjev, E. M. *Eur. Phys. J. E* **2001**, *4*, 21.

Table 1. Radius R and Polydispersity of the PMMA-PSA Particles, As Determined by Dynamic Light Scattering

source	R , nm	polydispersity
University of Edinburgh	250	0.04
University of Edinburgh	150	0.04
Van't Hoff Laboratory	100	0.05

particles. Although, as we shall see later, there is a significant difference in colloid aggregation and properties between bigger and smaller particles, one should always keep in mind a possibility that a different source of particles could have an effect.

Sample Preparation. We followed the preparation procedure outlined in refs 13 and 14. In short, dried particles were added at room temperature to a measured amount of liquid crystal. Subsequently, the temperature was raised well above the nematic transition temperature (to about 45 °C), and the sample was subjected to ultrasound in order to disperse the particles in the isotropic phase of 5CB. The samples were then stored at about 45 °C on a shaking device to ensure their homogeneity. For comparison, some of the preparations were done at high temperature, entirely within the isotropic state of the liquid crystal, but no substantial differences were recorded in the experimental results, which could be attributed to the difference in the preparation procedures. All experiments reported in this paper were performed at a constant particle concentration of 5 wt %.

Methods. Thin films of the colloid sandwiched between two glass slides were inspected under crossed polarizers using a Zeiss Axioplan optical microscope. The phase behavior of the pure 5CB and its mixtures with particles was studied by differential scanning calorimetry (DSC, Perkin-Elmer Pyris 1). The thermal protocols matched those of the rheological studies (see below). Mechanical properties of the system were studied on a dynamic stress rheometer (Rheometrics Ltd). Samples were loaded on the preheated rheometer stage at high temperature after ultrasonic excitation to ensure they were well dispersed and had not undergone a phase transition to the nematic state at any stage before loading. This ensured reproducible sample history and proved to be rather important, as the measured values of the storage modulus depended on whether the sample had been in an aggregated state prior to the measurement and, if so, for how long. The upper plate of the rheometer was then lowered to form a parallel plate geometry with a gap of 0.5 mm. The sample was left for thermal equilibration for several minutes and then subjected to oscillating shear of low frequency (2 Hz). This returned the rheological response of a simple isotropic liquid, hardly modified by a small amount of homogeneously dispersed particles. The storage and the loss moduli of the sample were then continuously monitored during cooling (from ~40 to ~17 °C) and subsequent heating (back to ~40 °C) with a linear temperature ramp. The temperature control was provided by a thermal bath, coupled to the rheometer, controlled by and directly reporting to the software. By this protocol, we were able to follow the change in the mechanical properties of the system during the formation and consolidation of the cellular structure.

Results

Cellular Structure. An illustration of the cellular structure formed in the sample after quenching from 45 °C to room temperature is shown in Figure 2a. Here, the sample was sandwiched between two glass slides to form a thin and transparent film. Since the bulk aggregated colloid is opaque, it is not possible to observe its structure in a thick sample by light microscopy (confocal microscopy, however, was used successfully to image the interior of three-dimensional samples¹⁴). The general morphology of the open cellular structure is evident from this image, with PMMA particles densely aggregated in thin interfaces and the 5CB nematic phase filling the cells. The average cell size is compatible with the one reported earlier for this particle concentration (the inverse proportionality of cell size and concentration has been established in ref

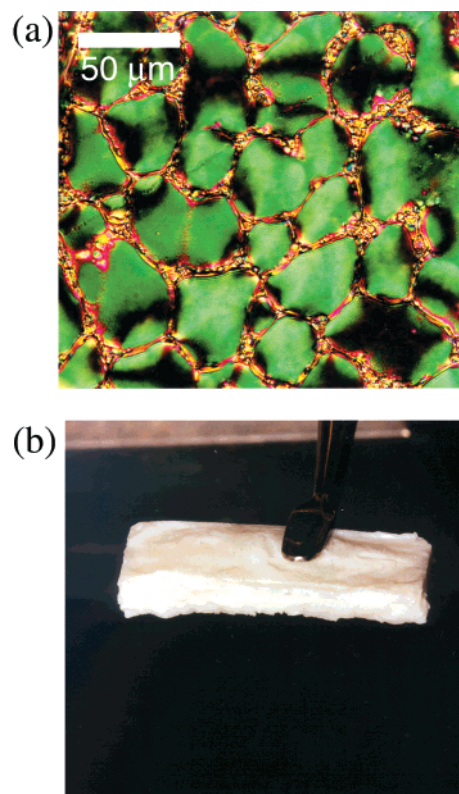


Figure 2. (a) Polarized microscopy image of the cellular structure formed in the liquid crystal colloid (in a thin film). (b) Photograph of the aggregated solid colloid sample demonstrating its mechanical strength and self-supporting ability.

14). Characteristic four-branch birefringence patterns indicate that the pure nematic liquid inside most cells has a director field consistent with topological charge of +1, being confined by anchoring on cell walls (the same dimensionless parameter, WL/K now with L the cell size, controls the topological state of the director field; it is clearly large at $L \sim 30\text{--}50\ \mu\text{m}$).

One could distinguish several stages of cellular structure formation during the aggregation in the system on cooling. First, at high temperature ($T > T_{\text{NI}}$) the system is in the isotropic state and the particles are evenly dispersed in the liquid phase. Upon lowering the temperature below the isotropic-to-nematic transition, the nucleation of the nematic phase begins. Although this phase transformation is of first order, it is known as a “weak first-order” transition¹⁶ with an important role of nematic fluctuations above the clearing temperature T_{NI} . During their nucleation and growth, the nematic regions increase in size, expelling the colloid particles to the surrounding isotropic regions, and the system effectively phase separates. The particles are restricted to the boundaries between the nematic droplets, where their concentration is increased. In this way, the walls of the cellular structure are constituted (see Figure 2a). Further decrease of the temperature strengthens the walls even more, due to the effective pressure created by the nematic mean field.¹⁵ As we shall see later, the aggregated colloid shows a high storage modulus ($G' \sim 10^3$ to 10^6 Pa, depending on the conditions), which makes its linear elastic response close to that of natural rubbers. Thus, the material behaves as a soft solid, well able to sustain its shape and its own weight (Figure 2b). Although it is obvious that the system is in a metastable state, this structure could stay intact

(16) Pikin, S. A. *Physica A* **1993**, 194, 352.

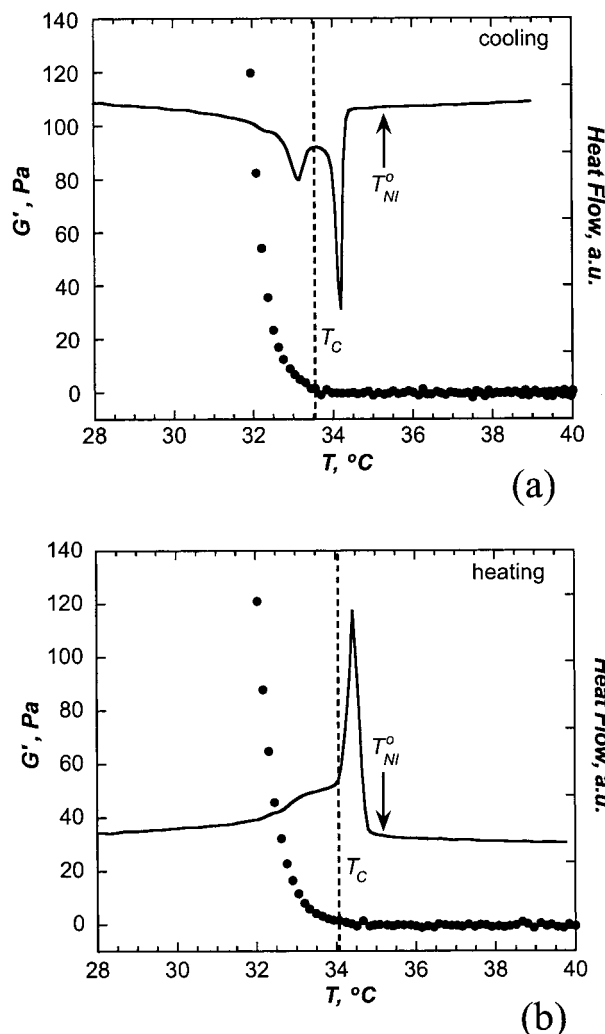


Figure 3. Differential scanning calorimetry (solid curve) and storage modulus (solid circles) of the liquid crystal colloid on cooling (a) and heating (b). Cooling rate 0.8 °C/min; heating rate 0.86 °C/min; particle concentration 5 wt %; particle radius 150 nm. T_{NI}^o is the nematic-to-isotropic transition temperature of the pure nematic LC, and T_c is the temperature at which G' begins to increase at cooling or vanishes at heating.

for a long period of time, due to the high energy barriers associated with cell wall disruption.¹⁴

Phase Behavior. Our first aim was to probe the phase behavior of the liquid crystal colloid. Figure 3 represents a typical DSC signature at a constant cooling and heating rate, plotted together with the corresponding data on the mechanical response of the system. We find that plotting the two effects together reveals much information about the system behavior. Two points should be noted concerning the results from differential calorimetry. The first is the obvious shift of the phase transition(s) toward lower temperatures as compared with that for the pure nematic LC. The pure 5CB showed a first-order phase transition with an exothermal latent heat peak at 35.3 °C on cooling. A sample doped with 5% colloid particles has its (first) transition temperature around 34.4 °C. This is to be expected because of disruptions of nematic order by particles, and the linear dependence of the transition temperature on the particle concentration has already been demonstrated.¹⁴ The second effect is the appearance of a two-peak structure indicating the existence of two subsequent, but different, first-order transitions (see Figure 3a). On cooling, immediately after the second transition takes place, the structure begins to solidify,

Table 2. Comparison between the Temperatures at the Onset of the First (T_{NI}) and Second (T_2) DSC Signals at Cooling with the Temperature at the Onset of the G' Rise (T_c) for Systems of Different Particle Sizes (R)^a

R , nm	T_{NI} , °C	T_2 , °C	T_c , °C
250	34.4	33.7	33.7
150	34.4	33.5	33.4
100	34.6	34.3	33.6

^a Cooling rate 0.8 °C/min. Particle concentration 5 wt %.

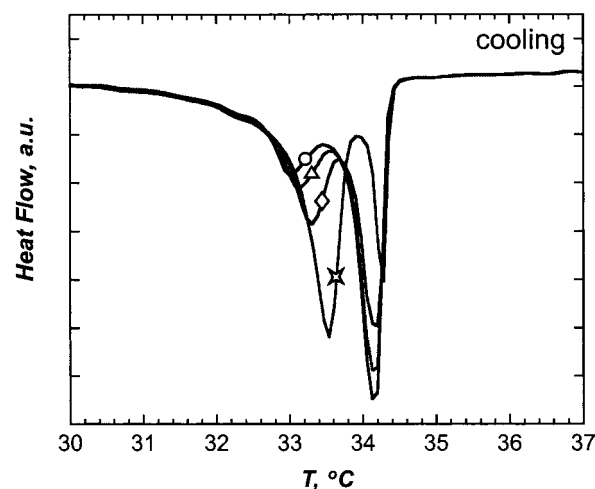


Figure 4. Results of four consecutive DSC scans of the system through its phase transition region. Only the cooling parts of the cycles are shown. Cooling rate 0.8 °C/min; particle concentration 5 wt %; particle radius 250 nm. Star, diamond, triangle, and circle label the first, second, third, and fourth scans, respectively.

and the storage modulus increases steeply (Figure 3a). Careful comparison between the DSC signals and the G' -temperature response shows that the low-frequency modulus $G'(\omega=2\text{Hz})$ begins to increase at a temperature T_c which corresponds to the onset of the second exothermic peak on the thermogram (see Table 2).

The behavior of the system during heating is analogous (Figure 3b), even though the lower-temperature DSC peak is less pronounced. When the melting of the nematic phase is approached, the storage modulus gradually decreases and vanishes at the temperature 34.1 °C for the case of Figure 3b, which corresponds to the temperature at which the lower-temperature phase transition ends. These results seem to hint that the lower-temperature phase transition is related to the onset of the rigid structure formation in our system. To further clarify the phase behavior of the system, we performed an additional experiment. In this case, a sample was cycled through the two-phase transitions four times, without allowing it to redisperse at high temperature. Figure 4 shows the result, where only the cooling parts of temperature scans are presented. As can be seen, the onset of the first phase transitions hardly changes with every successive cycle. From the sequence of plots, it appears that the second transition point, T_2 , is also constant. The relative intensity of the peaks, however, varies significantly for each subsequent cooling cycle and shows a clear trend: the first (higher temperature) peak increases and the second (lower temperature) one decreases with every cycle. Quantitative evaluation shows that the total area of the two peaks, giving the total enthalpy of the transition, remains constant and fairly close to that of the pure liquid crystal. On the basis of these observations, we could safely make the conclusion that both peaks are due to the same isotropic-to-nematic transition of the liquid crystalline

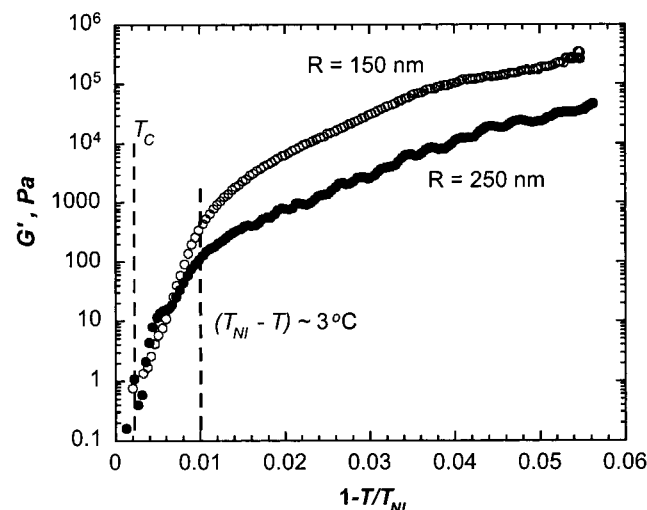


Figure 5. Dependence of the storage modulus of the aggregating liquid crystalline colloid on relative temperature during cooling, for two different particle sizes. Here T_{NI} is the first (higher) transition temperature, as determined by DSC. The first dashed line shows the temperature at the onset of the G' rise, T_c , whereas the second one indicates approximately the end of the initial stage of the rigid structure formation at about 3 °C below T_{NI} . Cooling rate 0.8 °C/min; particle concentration 5 wt %. Particle radius 150 nm (open circles) and 250 nm (solid circles).

matrix, only taking place in two stages. Further corroboration of this conclusion could be found in ref 14, where, for a similar system, the peak area decreased with the increase of the particle concentration, which is to be expected if the whole thermal effect is produced by the LC alone. Later, in the Discussion, we shall argue how all the observations of the phase behavior and the mechanical response of the system could be put together in a tentative dynamic picture of the structure formation.

Effect of the Particle Size. Next we examine the dependence of the storage modulus of the system, G' , on the temperature for two different particle sizes. Figure 5 shows a typical result for two particle radii, 150 and 250 nm. Generally, two different regimes are observed. Initially, G' rises steeply during the structure formation close to the isotropic-to-nematic transition temperature. This stage ends at about $(1 - T/T_{NI}) = 0.01$, that is approximately 3 °C below the temperature of the first transition T_{NI} , and a crossover into the second regime is observed, which appears in Figure 5 as an increase with a different slope (note the semilogarithmic plot axes). The increase of rigidity during the consolidation of the already established cellular structure is most probably due to the increased "nematic pressure" that the nearly pure liquid crystal in each cell exerts on the walls as the nematic order parameter increases. The mechanical stabilization of the system is impressive, with G' reaching values on the order of several times 10^5 Pa.

The effect of the particle size is readily noticeable. In the initial stage, the G' increases are similar for the two particle sizes. Later, we shall confirm this trend for the third, much smaller particle size (see Figure 7). This quite remarkable observation finds its explanation in the specific interparticle forces acting in the LC medium (we consider this situation in the Discussion). During the second regime, smaller particles produce a more rigid structure, with a difference in the storage modulus of about an order of magnitude.

Effect of the Cooling Rate. The rate of cooling of the initial isotropic mixture has a strong effect on the resulting

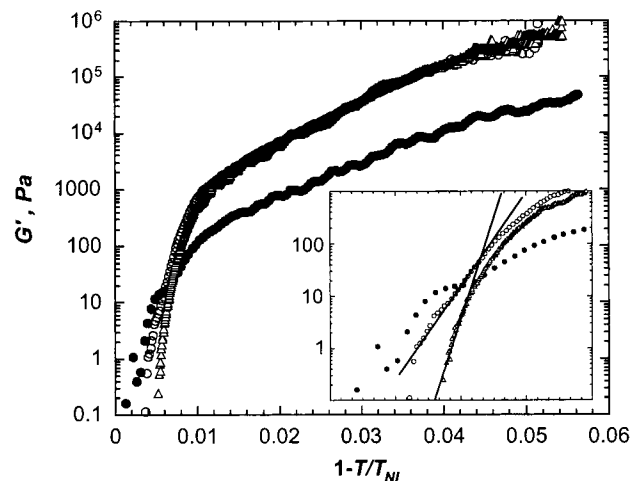


Figure 6. Dependence of the storage modulus on relative temperature during cooling for three different cooling rates. Particle concentration 5 wt %; particle radius 250 nm. Cooling rates 0.8 °C/min (solid circles), 0.3 °C/min (open circles), and 0.1 °C/min (triangles). The inset shows a magnified view of the initial stage of structure formation (the straight lines are only guides to the eye).

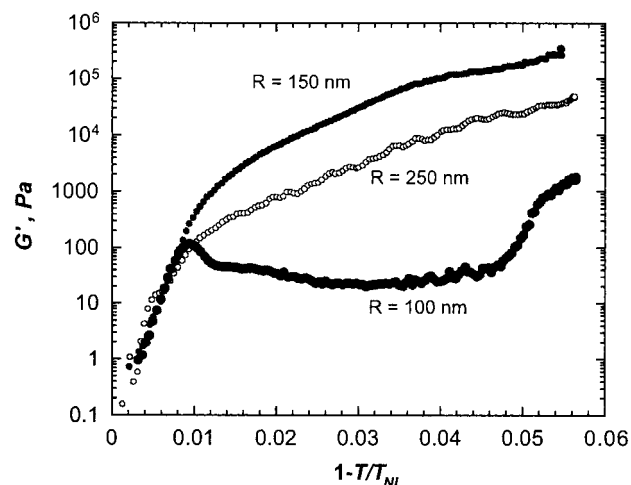


Figure 7. Dependence of the storage modulus on relative temperature during cooling for a colloid containing very small particles. Cooling rate 0.8 °C/min; particle concentration 5 wt %; particle radius 100 nm (solid circles). Data from Figure 5 are also included in this figure for comparison (small solid circles for $R = 150$ nm and small open circles for $R = 250$ nm).

mechanical properties, as illustrated in Figure 6. There, the temperature dependence of G' at three different cooling rates for identical particle radii (250 nm) is presented. Again, the two regimes, the initial cellular structure formation and the subsequent consolidation, are clearly distinguishable. The change of the cooling rate has a twofold effect. On one hand, the overall rigidity of the system is enhanced by about an order of magnitude when the cooling rate is decreased from 0.8 to 0.3 °C/min. A further decrease of the cooling rate to 0.1 °C/min has little effect on the low-temperature regime. On the other hand, the decrease of the cooling rate delays the onset of the structure formation and causes a steeper initial increase of G' (see the inset of Figure 6). This observation is in accordance with the DSC experiments: it appears we were to observe a discontinuous jump in G' , from zero to about 10–100 Pa, which has been masked by the aggregation kinetics.

Very Small Particles. As we have demonstrated above, smaller particles produce more rigid structures. This

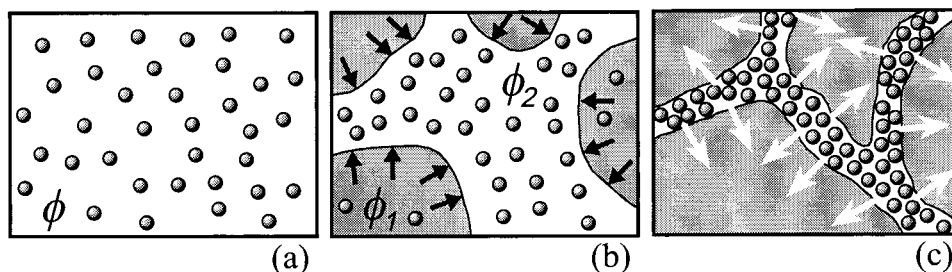


Figure 8. Schematic representation of the phase behavior of the LC colloid upon cooling: (a) Even dispersion of particles in an isotropic liquid at high temperature ($T > T_{NI}$); (b) intermediate state of the phase-separated system; black arrows denote the "nematic pressure" exerted by the liquid crystalline fraction (shaded areas) on the more concentrated colloid regions; (c) lower temperatures and respectively higher "nematic pressure" cause the swollen wall structure collapse and release of the remaining mesogenic liquid (white arrows).

motivated us to perform experiments with even smaller particles. A typical and reproducible result for a particle size of 100 nm is shown in Figure 7, along with the data from Figure 5 for comparison. As can immediately be seen, the G' rise is independent of the particle size in the stage of the initial establishment of the rigid structure. However, the observed trend at lower temperatures is different for the smallest particles (100 nm). The structure yields and is partially disintegrated at $G' \sim 100$ Pa, when the stress reaches a value just above 1 Pa.¹⁷ Rheological experiments on concentrated suspensions of the same PMMA-PHSA particles have shown¹⁸ that small particles (of diameter below 84 nm) behave as soft objects rather than hard spheres. This is due to the deformability of the grafted PHSA polymer, whose volume becomes a considerable part of the effective particle volume for such small particles. We could speculate that the partial structure disintegration in our case (Figure 7) could be due to the similar nonsolid sphere behavior of the particles condensed in the cell walls. One should, however, bear in mind that the differences might be due to the different particle sources as well. With a further decrease of the temperature and corresponding increase of the nematic order parameter, the structure is consolidated once again and G' reaches a respectable value between 10^3 and 10^4 Pa (see Figure 7).

Discussion

In this section we would like to address the important questions about the phase behavior of the LC colloid and the effect of the particle size on the mechanical properties of the system.

Let us reiterate the basic observations with respect to the phase behavior of the liquid crystalline colloid. The single first-order nematic-to-isotropic transition in the pure 5CB is split into two first-order transitions in the colloid. As we have shown (see Figure 4 and its analysis of total peak areas), both thermal anomalies, although observed at different temperatures, are caused by the nematic transition of the liquid matrix. The mechanical stabilization of the system, first signaled by the rise in G' , is triggered by the second, lower-temperature transition. These facts allow us to propose the following tentative picture of the aggregation process taking place on cooling. At high temperature, above the nematic transition, the particles are dispersed evenly in the isotropic liquid (Figure 8a). Upon decreasing temperature, the system undergoes phase separation into two phases of different

particle concentration. The driving force for this effect is, essentially, the nematic fluctuations in the isotropic phase just above the isotropic-to-nematic transition point of a given homogeneous colloid. Since this temperature is below T_{NI} , the system can gain free energy by locally reducing particle concentration and allowing the low-concentration regions to become nematic. Consequently, the liquid in the low-concentration phase of the separated mixture undergoes a nematic transition, at the temperature T_{NI} , manifested by the first peak in the thermogram. Now there are two coexisting phases, a nematic colloid of low particle concentration ϕ_1 and a more concentrated ($\phi_2 > \phi_1$) coexisting isotropic phase (Figure 8b). The concentrated isotropic phase could be considered as highly swollen "walls" of the future cellular structure to be formed upon further temperature decrease. Since the liquid in the other phase is already in the nematic state, it starts to exert a force on the border with the surrounding swollen isotropic structure, caused by the nematic mean field, to which we have referred several times as "nematic pressure". By this we mean the effective pressure across an interface between nematic and isotropic phases. It can be expressed as a force $-\Delta F(N-I)/\Delta x$ on displacing the interface by Δx , divided by its area, making the nematic pressure equal to the difference in thermodynamic free energy densities between the nematic and isotropic phases, $\Delta P = -\Delta F(N-I)/V$. Although we are far from suggesting that a simple Landau theory is a good description of the nematic-to-isotropic phase transition, for illustration purposes we could use its results for free energy density: the nematic pressure increases as $\Delta P \approx (\text{const})Q^2 \sim (\text{const})|T - T_{NI}|$, where $Q(T)$ is the nematic order parameter. It is reasonable to assume that, upon decreasing temperature to a lower value $T = T_2$, the system reaches a critical order parameter $Q(T_2) = Q^*$, at which the nematic pressure is high enough to make the swollen structure collapse. During this compaction, the rest of the isotropic liquid is expelled into the surrounding nematic region, where it undergoes a nematic transition, hence the second, low-temperature peak observed in the thermogram (see Figure 8c, where the expulsion of the isotropic liquid is marked by white arrows). The total area under both DSC peaks is, thus, proportional to the total amount of nematic material and remains constant even though different proportions of this material experience the transition at different moments. The whole structure is stabilized mechanically, because densely compacted walls are in the colloidal solid state, which causes the observed increase of the storage modulus. Further temperature decrease merely strengthens the structure by further increasing the nematic pressure. It is easy to reconcile the suggested picture with the DSC data in Figure 4, as well. The important feature of the experiments reported in Figure

(17) In contrast, the stress for the other systems in the fully aggregated state was about 60 Pa for $R = 250$ nm and above 100 Pa for $R = 150$ nm.

(18) Frith, W. J.; Mewis, J.; Strivens, T. A. *Powder Technol.* **1987**, *51*, 27.

4 is that the colloid is cycled several times through its nematic transition, but it was kept only for a short time at high temperature, so that the cell walls were obviously not fully disintegrated. The walls are strengthened on cooling and partially swollen on heating, but with every cycle the amount of isotropic liquid swelling the walls decreases. As a result, smaller amounts of liquid are expelled during the collapse of the walls at T_2 on every successive cooling, so that the area under the second peak decreases to complement the respective area increase of the first peak.

As we have seen, there are two distinct regimes of the low-frequency storage modulus increase when the temperature is lowered steadily. At first, just after the isotropic-to-nematic transition, G' raises steeply. Figure 6 clearly shows that this initial region of cellular structure formation is dominated by the aggregation kinetics. Therefore, the time of aggregation determines the outcome value for $G'(T)$. The storage modulus, as evident from Figure 5 and especially Figure 7, is independent of the particle radius. At first sight this result seems surprising, since it is clear that the drag force exerted on a particle in a liquid medium must depend on the particle radius and would affect, eventually, the colloid aggregation time. One should not forget, however, that the attraction force between the particles is mediated by the liquid crystalline matrix. As an estimate of a typical aggregation time in the system, one could use the time necessary for two particles, suspended in an LC medium, to come into contact with each other. In our case of a weak relative anchoring, $WR/K \ll 1$, the attraction force is calculated in ref 19 to be $F \sim W^2 R^6 / K d^6$, where d is the distance between two interacting particles. If we assume that the drag force is roughly $F_{\text{drag}} \sim 6\pi\eta Rv$, where η is the characteristic viscosity and v is the particle velocity, the aggregation time τ can be obtained by balancing the two forces, as done in ref 19. The result is $\tau \sim \eta K / W^2 (\phi^{-7/3} - \phi_c^{-7/3})$, where ϕ is the initial concentration of the colloid and ϕ_c is the maximal close-packing volume fraction. By this argument, the initial colloid aggregation time is independent of the particle size, and therefore, the storage modulus in the region dominated by the aggregation kinetics should also be independent.

During the second, low-temperature regime, the rigidity of the system increases considerably (the storage modulus rises up to 10^6 Pa) and this value depends on the particle size, in contrast to the initial stage. Model considerations show that the average energy density of an even highly unfavorable situation of homogeneously dispersed particles in a nematic liquid cannot account for the huge values of the observed storage modulus.¹⁵ The origin of this considerable rigidity has to be sought in the essentially solid state of random close packing or even crystalline nature of densely packed walls of the open-cell structure.²⁰ In particular, depletion interactions between particles could account for the increase of G' with decrease in the particle size. After the phase separation process, the particles are in close contact with each other. Each contact between two particles would reduce the volume accessible for the remaining molecules of 5CB, thereby reducing the surface energy of the particles. This effect provides a restoring force, which can be considered as an effective surface tension of the wall, γ_d . It is found to be¹⁵ $\gamma_d \approx \beta \gamma_0 a \phi_c^2 / R^2$, where β is a numerical coefficient, γ_0 is

the interfacial tension of the boundary between grafted polyhydroxystearic acid and biphenil oil, a is the size of the molecule of the suspending liquid, ϕ_c is the maximal particle volume fraction at random close packing in the densely compressed cell walls, L is the characteristic mesh size of the cellular structure, and R is the radius of the particle. Using this approximate expression, one could estimate the ratio of the storage moduli ($G' \approx \gamma_d / L$) for two different particle sizes, $G'(R_1) / G'(R_2) \approx R_2^2 / R_1^2$. Taking $R_1 = 150$ nm and $R_2 = 250$ nm, we obtain $G'(R_1) / G'(R_2) \approx 2.8$, in qualitative agreement with the experimental data. Thus, the depletion interaction between the suspended particles may account, at least in part, for the increase of the storage modulus in systems of smaller particles. We also note that this depletion effect is likely to be more pronounced at higher undercoolings, when the walls are densely packed due to the increased nematic pressure. In contrast, it would play only a minor role during the initial aggregation stage, hence the crossover from size-independent to size-dependent storage modulus on cooling.

The rise of the storage modulus with the decrease of temperature, however, cannot be accounted for by this depletion effect. It should be attributed to the increasing order parameter in the nematic liquid, which creates increasing temperature dependent nematic pressure. This effect, however, has not been considered theoretically so far; the closest analogy one could find is in theories of granular matter compacted under increasing pressure or gravity.

Conclusions

We have studied the phase behavior and rheological properties of a low-concentration liquid crystalline colloid, capable of forming cell-like structures by expelling the particles into densely packed thin walls. We have demonstrated that, upon quenching the system below the clearing point of the liquid crystalline matrix, it undergoes two consecutive first-order phase transitions, both attributed to the isotropic-to-nematic transition of different portions of the mesogenic liquid matrix.

Formation of cellular structure is triggered by the growing nematic order parameter $Q(T)$. At later stages, when the temperature of the sample is considerably lower than the clearing temperature, the structure is consolidated by the increasing nematic pressure exerted on the cell walls by the surrounding anisotropic liquid.

One of the most important results of the present study is the possibility to practically control the properties of the new material. This could be done in different ways, for example, by changing the size of the suspended particles, varying the cooling rate, or selecting a different LC matrix (in order to invoke a different nematic field strength). The optimal particle size appears to be around 150 or 250 nm. This value is limited from above, because of the requirement for the parameter WR/K to be small enough, and from below, because of a possible "soft" behavior of smaller particles. By varying some of the system parameters, we have demonstrated the possibility to reach very high values of the storage modulus, up to 10^6 Pa (see Figures 5 and 6).

Possible future work may include other types of suspending liquids with broken symmetry, in particular lyotropic phases.²¹ Further theoretical considerations are necessary, as well, to understand quantitatively the phase behavior, aggregation kinetics, and rheology of these systems.

(19) Ruhwandl, R. W.; Terentjev, E. M. *Phys. Rev. E* **1997**, *55*, 2958.

(20) Unlike the case of the open-cell foams, where the elastic properties of the cellular structure are mainly due to the relative density of the foam: Gibson, L. J.; Ashby, M. F. *Cellular solids. Structure and Properties*; Pergamon Press: Oxford, 1988; pp 127–129.

(21) Koehler, R. D.; Kaler, E. W. *Langmuir* **1997**, *13*, 2463.

Acknowledgment. We would like to thank W. C. K. Poon and S. P. Meeker (University of Edinburgh) for valuable discussions and donation of particles. Some of the particles used in this study were supplied by the Van't Hoff Laboratory of Utrecht University, where they were synthesized by Mr. Klaas Groot. We appreciate the valuable discussions and assistance of S. M. Clarke, P. Cicuta, V. J. Anderson, and E. W. Kaler. This work has been supported by EPSRC UK.

Note Added after ASAP Posting

In the version of this article released ASAP on 4/10/2001, the equation for τ in the left column of the preceding page was incorrect. This was due to a production error. The correct version was posted on 4/13/2001.

LA0016470